ANALYZING THE EFFECT OF MULTI-CHANNEL MULTI-SCALE SEGMENTATION OF RETINAL BLOOD VESSELS

Ain Nazari[1], Mohd Marzuki Mustafa[2] and Mohd Asyraf Zulkifley[3]
Department of EESE, Faculty of Engineering and Built Environment, UKM, Bangi, Selangor, Malaysia
Faculty of Electrical and Electronic Engineering, UTHM, Parit Raja, Batu Pahat, Johor, Malaysia
E-Mail: ainnazari@siswa.ukm.edu.my

ABSTRACT

Retinal blood vessel segmentation is one of the important modules in developing an automated vessel detection system, which is used to pre-screen various types of disease. This paper proposes a segmentation technique for retinal blood vessel using multi-channel multi-scale edge detection method. Multi-channel approach is implemented because of more information can be extracted compared to a single channel. After that, multi-scale edge detection is applied to detect the blood vessels which vary in size from 1 pixel to 15 pixels width. The contrast is then improved through standardization of the original response image. Finally, binarization method is applied to remove the noise to get the final segmented retinal blood vessels. Simulation results show that blood vessels have been segmented accurately by using images from two publicly available databases, DRIVE and HRF. The best accuracy is 0.93 obtained from DRIVE database while the finest precision is 0.94 obtained from HRF database. Meanwhile, the highest sensitivity obtained is 0.61 from DRIVE database whereas the best specificity is 0.98 based on HRF database. In conclusion, an accurate information of retinal blood vessel condition will be very beneficial to pre-screen numerous diseases.

Keywords: retinal image, multi-channel, multi-scale, segmentation.

INTRODUCTION

An automated analysis of retinal blood vessels properties is an important task, which are beneficial for disease progression tracking, treatment evaluation, clinical study investigation and also for biometric authentication. Retinal blood vessel information is preffered because of its uniqueness that vary from one individual to the others that makes the identification process easier. It is also suitable for early abnormalities screening that related to eye conditions, especially by analyzing the retinal vascular structures. There are two types of abnormality associated with the eye (Thesis, 2006): lifestyle related disease and being disease of the eye. Some examples of lifestyle related diseases are arteriosclerosis, diabetes, stroke, and hypertension. On the other hand, some examples of being a disease of the eye are blepharitis, cataract, conjunctivitis, and glaucoma (Hayashi *et al*. 2001).

Segmentation of the vasculature is the most importance step in retinal fundus image analysis. Moreover, accurate vessel segmentation is a challenging task due to the variability of vessel width, shape, brightness, existence of noise, and unstable contrast between vasculature and background. Various methods have been proposed on the segmentation of retinal blood vessel, where it can broadly classified into thresholding method (Xu and Luo, 2010) and edge detection(Lee, 2012).

For the thresholding method, it aims to classify each pixel in the fundus image into two groups: vessel and non-vessel. Usually, this method results in a binary image output. Various types of threshold have been researched from the basic Otsu method (Nayebifar and Abrishami Moghaddam, 2013) to the local and advance adaptive threshold (Martinez-Perez, Hughes, Thom, Bharath, and Parker, 2007; Winder, Morrow, McRitchie, Bailie, & Hart, 2009). In practice, an adaptive thresholding method capables to extract the segmented retinal blood vessel from grayscale image (Kirbas and Quek, 2003) that will influence the performance measures of the segmentation (Heneghan, Flynn, O'Keefe, and Cahill, 2002). The main drawback of this approach occurred when the value of the threshold is too high, which will result in miss detection of important vessel. While, a small threshold value will produce a lot of noisy detection.

Method in (Ricci and Perfetti, 2007) segmented the retinal blood vessel by using simple line detection. A similar approach has also been described in (Nguyen, Bhuiyan, Park, and Ramamohanarao, 2013) with improved multi-scale line detection for variable scale input. However, both of the papers used only a single channel which is the green channel of RGB retinal fundus image. They validated the proposed algorithm by using DRIVE and STARE database, respectively. In addition, (Kong, 2006) segmented the retinal blood vessel using multi-scale analysis using adaptive tracking threshold and Gabor morphology filtering. The rest of the paper is organized as follows. Section I provides introduction and literature review of the vessel segmentation. Details on the proposed method are described in Section II. Section III presents the experimental results based on DRIVE and HRF database. Finally, the conclusion of the paper is explained in Section IV.

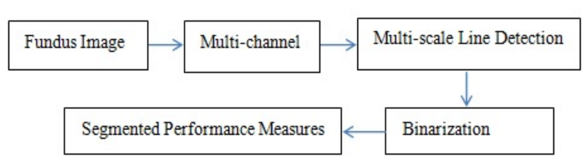

Figure-1. Block diagram showing the steps of the proposed technique.

VOL. 10, NO. 18, OCTOBER 2015 ISSN 1819-6608
ARPN Journal of Engineering and Applied Sciences

www.arpnjournals.com

Figure-1 delineates the main steps involve in the proposed technique. There are five main steps regarding automated segmentation of retinal blood vessels which are explained in the following subsections.

Multi-channel

RGB color model comprises of three color channels, which are red, green and blue (Parveen, 2010). In fundus image, green channel has the best contrast between blood vessel and the background. Meanwhile, red channel has a low contrast and often saturated that results on a lot of bright pixels. The blue channel is a very noisy component because of poor dynamic range. However, it does not mean that red and blue channels do not contain any significant information just that blood vessels are more suitable to be presented by green channel because of the highest contrast (Walter *et al.* 2007). As a result, this paper proposes multi-channel approach instead of favoring green channel only. Each channel is treated separately, where red, green and blue channels will undergo the same process. Each channel will be map to 8-bit gray-scale image for red, green and blue channels, which later will be filtered to reduce the noise (Meshram and Pawar, 2013). The grayscale representation strengthen the presence of retinal blood vessel which is the darker region. Then, an inverted form will be used, so that the detected blood vessles will be represented by bright pixel while the surrounding will be detected as dark pixel for each channel.

Multi-scale line detection

Firstly, the vessel is modelled through its width, W which is set to 15 pixels where the normal width is around 7 to 8 pixels. A kernel of 15×15 pixels is built to evaluate the average gray level, I_{avg}^{W} through convolution process. The average gray level of the pivot pixel is assessed along 12 lines that pass through the center pixel at 12 different orientations with the angle resolution of 15º. Figure-2 shows the lines detector with L=5 and W=15 that produced 12 lines of 5 pixel length. L is the length scale factor where all of them are positioned in a kernel of 15×15 pixels. The line with the highest value among the average gray level will be called "successful line" and denoted as I_{max}^{L}. Subsequently, the value of L vary from 1 to 15 with a step size of 2 that needs to fulfill the condition of $1 << L << W$. The condition will result in 8 scales where the range of vessel's diameter is to be expected. Figure-3 illustrates different scales of length for $L= 3, 5$, and 11 pixels. It clearly shows the progressive blurring process of the image gradually proportional to the scale factor. The main purpose of using the shorter length line detection is to avoid the inclusion at the vessels pixels, in order to get the correct vessel's detects especially at the crossovers point. The proposed algorithm uses line detector that has a variable length of the aligned lines. The line response at each pixel is defined as equation (1). The initial parameters of W is 15 and L is 3 to get the line response.

$$R_W^L = I_{\max}^L - I_{avg}^W \tag{1}$$

However, the original response obtained by the edge detector at each scale is in a limited scale. As a result, it produces a low contrast output between the vessels and the background. In order to increase the contrast,the standard response is implemented to the original response image by using standard deviation and zero mean of the image. The goal is to keep the intensity value relatively the same but it extends to the broader range. The standardized response value is defined in equation (2), where R is the original response, R_{mean} and R_{std} are the mean and standard deviation of the original response, respectively. After that, the standardized image is measured for each channel or red, blue and green channel. Lastly, from the standardized image, the maximum, minimum and average pixels values from the combination of red, green and blue channels are measure are defined in equation (2) – (4).

$$R_{stdz} = \frac{R - R_{mean}}{R_{std}} \tag{2}$$

$$Maximum = \max\ (R_{stdz(r)}, R_{stdz(\mathrm{g})}, R_{stdz(\mathrm{b})}) \tag{3}$$

$$Minimum = \min\ (R_{stdz(r)}, R_{stdz(\mathrm{g})}, R_{stdz(\mathrm{b})}) \tag{4}$$

$$Average = avg\ (R_{stdz(r)}, R_{stdz(\mathrm{g})}, R_{stdz(\mathrm{b})}) \tag{5}$$

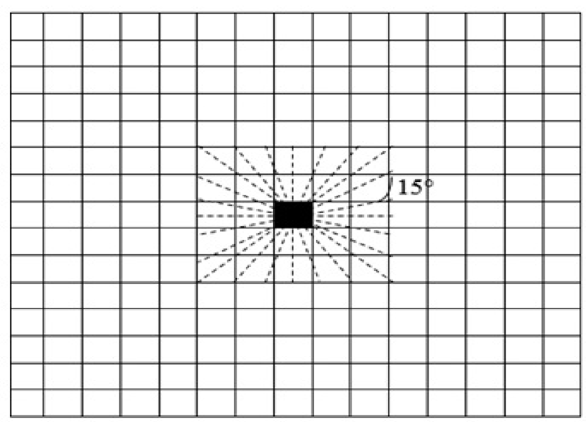

Figure-2. Twelve lines of length W pixels oriented at 12 different directions with angular resolution of 15º.

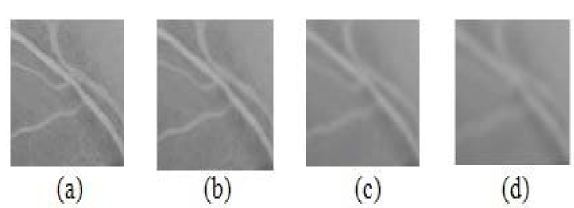

Figure-3. The different scales of length (a) original image (b) Length=3 (c) Length=7 (d) Length=11.

VOL. 10, NO. 18, OCTOBER 2015 ISSN 1819-6608
ARPN Journal of Engineering and Applied Sciences

www.arpnjournals.com

Figure-4 illustrates the original response image against the standardized image for DRIVE and HRF databases. It clearly shows that the standardized image produces better vessels segmentation compared to the original response.

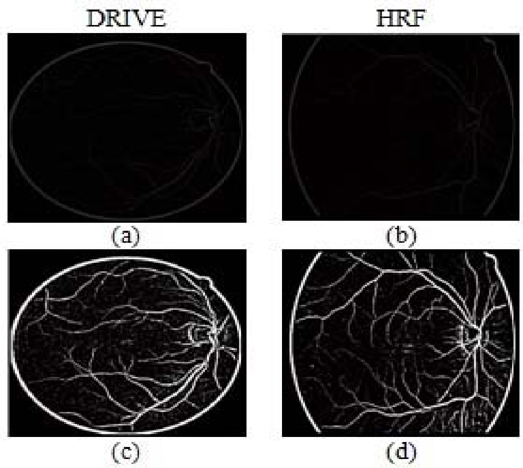

Figure-4. The differentiate between original response image with the standardized image (a)-(b) The original response image (c)-(d) The standardized image.

Binarization

A binary output mask of the segmented image is generated through thresholding method. The binarization process is done by setting a heuristic threshold of 0.56. This value is chosen by observing and training 20 images from DRIVE database. However, threshold is crucial because a small threshold will induce more noises while a high threshold will make the detection less sensitive. This binarization process will categorize every pixels into two groups as defined in equation (3). The same threshold value, t = 0.56 is then used to segment all images in DRIVE and HRF database.

$$\mathrm{G}(x, y) = \begin{cases} 255 & G1(x, y) \geq t \\ 0 & G2(x, y) < t \end{cases} \tag{6}$$

Performance measures

The performance of the algorithm is evaluated by comparing the segmented image with manually traced ground truth data by the experts. The segmentation performance is assessed using accuracy, precision, sensitivity and specificity measures. Accuracy (ACC) is the ratio of the total numbers of correctly classified pixel to the total number of pixels in the image. Meanwhile, precision emphasizes on the proportion of identified vessel pixels that are true vessel pixels over true positive detection. Sensitivity is a measure of actual positives that are correctly segmented as vessel, whereas specificity measures the proportion of negatives that are correctly segmented as blood vessel. Consequently, there are four parameters that need to be evaluated, which are true positive (*Tp*), true negative (*Tn*), false negative (*Fn*) and false positive (*Fp*). *Tp* is a pixel that is listed as a vessel for both tested and ground truth data, meanwhile a pixel is labelled as *Tn* when vessel is not detected in both tested and ground truth data. *Fn* is specified if non-vessel pixel is stated in the tested data when actually the ground truth returns a presence of vessel, while a pixel is classified as *Fp* if the vessel is present in tested image but returns none in ground truth image. Table-1 summarizes the types of classification used for performance measure.

Table-1. Performance classification of blood vessel detection.

	Vessel present	**Vessel absent**
Vessel detected	True Positive (*Tp*)	False Positive (*Fp*)
Vessel not detected	False Negative (*Fn*)	True Negative (*Tn*)

$$Accuracy\ (ACC) = \frac{T_p + T_n}{T_p + T_n + F_p + F_n} \tag{7}$$

$$Precision\ (PPV) = \frac{T_p}{T_p + F_p} \tag{8}$$

$$Sensitivity\ (TPR) = \frac{T_p}{T_p + F_n} \tag{9}$$

$$Specificity\ (SPC) = \frac{T_n}{T_n + F_p} \tag{10}$$

RESULTS AND DISCUSSIONS

The proposed method is evaluated on two publicly available databases, Digital Retinal Images for Vessel Extraction (DRIVE) database (Staal, Abràmoff, Niemeijer, Viergever, and van Ginneken, 2004) and High Resolution Fundus (HRF) database (Nithya, 2014). Both databases contain a mask for each image to filter the background information. The challenges in manual masking process are caused by double boundaries that persist during image acquisition, illumination artifacts, as well as tags numbers and variant of field of view (Sofka & Stewart, 2006). Hence, by using automatic masking provided by the databases, the background can be properly removed. In this paper, forty images are selected that consist of 20 images from training set, and another 20 images for 1st manual test set from DRIVE database while 15 images have been sampled to evaluate from HRF database.

Figure-5 shows samples of segmented output for every step for two fundus images from DRIVE and HRF databases each. The steps that are illustrated start from the input fundus image until the segmented image of the blood vessels by assessing the maximum, minimum and average of the multi-channel input.

VOL. 10, NO. 18, OCTOBER 2015 ISSN 1819-6608
ARPN Journal of Engineering and Applied Sciences

Table-2. Performance measure results.

	Database	ACC	PPV	SPC	TPR
Max	DRIVE	**0.93**	0.79	0.97	**0.61**
	HRF	0.85	**0.94**	**0.98**	0.18
Min	DRIVE	0.90	0.75	0.97	0.5
	HRF	0.83	0.80	0.85	0.24
Avg	DRIVE	0.92	0.80	0.98	0.58
	HRF	0.83	0.93	0.98	0.17

Table-2 summarizes the performance of the system in terms of accuracy, precision, sensitivity and specificity. The results show that the proposed algorithm produces favorable results in accuracy for DRIVE database, while HRF database performs well in precision measure. On the other hand, both databases get for a high specificity measure. In addition, the sensitivity for DRIVE database returns a better performance compared to HRF database, with the difference is about half of them.

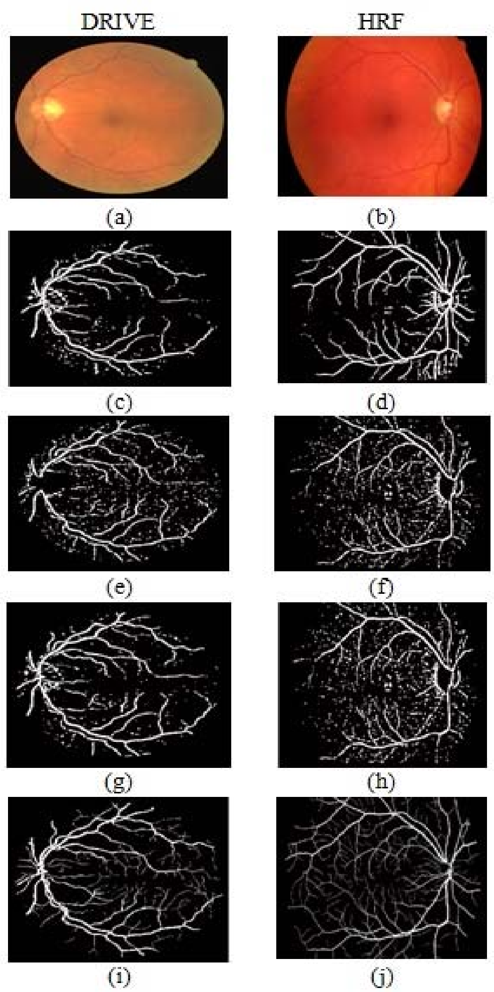

Figure-5. The retinal blood vessel segmentation (a)-(b) input images (c)-(d) Maximum method of multi-channel (e)-(f) Minimum method of multi-channel (g)-(h) Average method of multi-channel (i)-(j)ground truth image.

CONCLUSIONS

In conclusion, multi-channel multi-scale edge detection has been proposed to segment the retinal blood vessel. The performance of the proposed method is verified and validated by using two online databases, DRIVE and HRF. The results show that the proposed algorithm performs well for both databases. Therefore, the proposed algorithm can be a good base for blood vessel segmentation in many applications. As for the future work, the research will focus on improving the accuracy of the segmented output built upon the proposed method.

ACKNOWLEDGEMENTS

We would like to acknowledge funding from Universiti Kebangsaan Malaysia (ScienceFund: 06-01-02-SF1005) and Universiti Tun Hussein Onn Malaysia.

REFERENCES

[1] Hayashi J., Kunieda T., Cole J., Soga R., Hatanaka Y., Hara T. and Fujita H. 2001. A development of computer-aided diagnosis system using fundus images. Proceedings Seventh International Conference on Virtual Systems and Multimedia, pp. 429–438.

[2] Heneghan C., Flynn J., O'Keefe M. and Cahill M. 2002. Characterization of changes in blood vessel width and tortuosity in retinopathy of prematurity using image analysis. Medical Image Analysis, Vol. 6, No. 4, pp. 407–429.

[3] Kirbas C. and Quek F. K. H. 2003. Vessel extraction techniques and algorithms: A survey. In. Proceedings of Third IEEE Symposium on Bioinformatics and Bioengineering, pp. 238–245.

[4] Kong H. 2006. A New Approach to Automated Retinal Vessel Segmentation Using Multiscale Analysis, pp. 18–21.

[5] Lee T. H. 2012. Edge Detection Analysis. IJCSI International Journal of Computer Science Issues, Vol. 5, No. 6, pp. 1–25.

[6] Martinez-Perez M. E., Hughes A. D., Thom S. A., Bharath A. A. and Parker K. H. 2007. Segmentation of blood vessels from red-free and fluorescein retinal images. Medical Image Analysis, Vol. 11, No. 1, pp. 47–61.

[7] Meshram S. P. and Pawar M. S. 2013. Extraction of Retinal Blood Vessels from Diabetic Retinopathy Imagery Using Contrast Limited Adaptive Histogram Equalization, No. 3, pp. 143–147.

VOL. 10, NO. 18, OCTOBER 2015 ISSN 1819-6608
ARPN Journal of Engineering and Applied Sciences

www.arpnjournals.com

[8] Nayebifar B. and Abrishami Moghaddam H. 2013. A novel method for retinal vessel tracking using particle filters. Computers in Biology and Medicine, Vol. 43, No. 5, pp. 541–548.

[9] Nguyen U. T. V, Bhuiyan A., Park L. A. F. and Ramamohanarao K. 2013. An effective retinal blood vessel segmentation method using multi-scale line detection. Pattern Recognition, Vol. 46, No. 3, pp. 703–715.

[10] Nithya K. A. 2014. Classification of normal and abnormal retinal images using neural networks, Vol. 3, No. 9, pp. 3111–3115.

[11] Parveen N. R. S. 2010. Feature extraction on colored x-ray images by bit- plane slicing technique, Vol. 2, No. 7, pp. 2820–2824.

[12] Ricci E. and Perfetti R. 2007. Retinal blood vessel segmentation using line operators and support vector classification. Medical Imaging, IEEE Transactions on, Vol. 26, No. 10, pp. 1357–1365.

[13] Sofka M. and Stewart C. V. 2006. Retinal vessel centerline extraction using multiscale matched filters, confidence and edge measures. IEEE Transactions on Medical Imaging, Vol. 25, No. 12, pp.1531–46.

[14] Staal J., Abràmoff M. D., Niemeijer M., Viergever M. A. and van Ginneken B. 2004. Ridge-based vessel segmentation in color images of the retina. IEEE Transactions on Medical Imaging, Vol. 23, No. 4, pp. 501–509.

[15] Thesis M. 2006. Automatic diagnosis of diabetic.

[16] Walter T., Massin P., Erginay A., Ordonez R., Jeulin C. and Klein J.-C. 2007. Automatic detection of microaneurysms in color fundus images.

[17] Winder R. J., Morrow P. J., McRitchie I. N., Bailie J. R. and Hart P. M. 2009. Algorithms for digital image processing in diabetic retinopathy. Computerized Medical Imaging and Graphics : The Official Journal of the Computerized Medical Imaging Society, Vol. 33, No. 8, pp. 608–22.

[18] Xu L. and Luo S. 2010. A novel method for blood vessel detection from retinal images. Biomedical Engineering Online, Vol. 9, No. 1, p. 14.